Study of the Influence of Soluble Ions on Morphological and Microstructural Properties of Synthetic Ettringite

A. Lo Presti[1], G. Artioli[1], A. Bravo[2], F. Cella[2], T. Cerulli[2], M. Magistri[2]
[1]University of Milan, Italy; [2]MAPEI S.p.A., Milan, Italy.

Abstract

Ettringite ($Ca_6Al_2(SO_4)_3(OH)_{12}.26H_2O$) occurs as hydration product in most of cementitious systems. Even though the common habit is hexagonal-prismatic, different shapes and sizes are observed in bindings. During the first hours of hydration, shape and size of the ettringite crystals can be influenced by chemical composition of cement paste, affecting the setting behaviour. We think that ettringite properties are connected to the development of mechanical strengths of cementitious systems during early hydration stages.

Our aim was to study the influence of pH and concentration of different ionic species on morphology and microstructure of ettringite synthesized from solution of $Al_2(SO_4)_3$ and CaO under controlled conditions.

Analysis were carried out with ESEM-FEG and Line Profile Analysis (LPA) on XRD data. The latter were collected both using conventional X-ray sources and synchrotron radiation at the ESRF.

Results show a good correlation between morphology, measured as length/thickness ratio of ettringite crystals, and dimension of crystallites.

We also found some relation between synthetic model and real cementitious systems.

1. Introduction

Ettringite $Ca_6[Al(OH)_6]_2(SO_4)_3 \cdot 26H_2O$ approximately,   is   a   naturally occurring mineral but above all is a phase that typically forms during the early hydration stages of Portland cements.

Primary ettringite forms from tricalcium aluminate, $Ca_3Al_2O_6$ (C_3A) and calcium sulphate, added to Portland cement to prevent rapid setting and improve strength development, right after water addition, following the reaction:

$3\ CaO \cdot Al_2O_3 + 3\ CaSO_4 \cdot 2H_2O + 26\ H_2O \rightarrow 3\ CaO \cdot Al_2O_3 \cdot 3\ CaSO_4 \cdot 32\ H_2O$
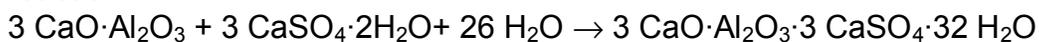
Ettringite crystallizes almost instantly when water is added and forms hexagonal-prismatic crystals.

The H_2O molecules are partly bound very loose into the ettringite structure. Due to this, the easy slit off of part of the water during drying or increased temperatures can be explained and, therefore, the existence of ettringite with different crystal water contents [1].

During the first hours of hydration, shape and size of the ettringite mainly change in dependence of the solution composition and due to this the setting behaviour is influenced [2].

The causes of many different forms in which ettringite appears are not yet fully explained. Some influencing factors seem to be the composition, the pH, the Ca^{2+} and SO_4^{2-} ions concentration into the growth solution [3,4,5,6,7] as well as the formation mechanism (through-solution mechanism or solid state reaction), the inclusion of foreign ions, etc.

Chartschenko [6] proposed a dependence of the length/thickness ratio of ettringite crystals on the pH value of the reaction solution.

Long, fiber-shaped crystals were formed at pH values between 10 and 12, but extremely microcrystalline ettringite was present at pH values above 13.0.

Investigation of the properties of ettringite that develops in minimal amount during the hydration process is difficult. For this reason a synthetic model is necessary to isolate and study only those reactions pertaining to the nucleation and growth of ettringite and the effects of environmental chemicals on those processes.

Several solution growth experiments were conducted using previously published methods: method of Struble and Brown [8] and the method of Mylius described in Taylor [9], but it was necessary to develop a new method of crystal growth for the present study, in order to obtain ettringite in well controlled environmental conditions.

A lot of chemical admixtures such as retarders, accelerant, plasticizers, superplasticizers are commonly added immediately before or during mixing to modify the properties of hardened concrete. It is important to know the effects of these chemicals on the formation and stability of ettringite.

As a matter of fact, it is assumed that there could be a relationship between ettringite characteristics (i.e. morphology) and the physical properties (rheology, mechanical strengths) of the hydrating cement paste.

In our opinion the knowledge of the crystallographic details of ettringite and of the kinetics of its formation in cementitious system is crucial to predict the physical behaviour of a given cementitious material.

We chose three different pH values for our synthesis: 10, 11, 12, to reproduce the starting pH value of the most common cementitious systems: calcium aluminate cement (CAC), ternary systems (CAC, OPC, sulphate), Ordinary Portland Cement (OPC) respectively.

We also synthesized ettringite maintaining a constant pH value and varying the salt concentration. Actually, we changed the ionic strength adding a different amount of calcium nitrate tetrahydrate, in excess with

respect to the stoichiometric ratio, in the starting solution, to obtain different conditions of $[Ca^{2+}]$ ranging from 0 to 16,9 g/l.

The influence of admixtures, and in particular superplasticizers, was tested adding them at the beginning of the reaction.

2. Experimental

2.1 Synthesis of ettringite

We synthesized ettringite in controlled environmental conditions.

To perform the synthesis, 10 ml of a water solution (40 g/l) of aluminium sulphate $(Al_2(SO_4)_316H_2O)$ previously prepared, is poured in a four-necked, round bottomed flask, where different amounts, according to the experiment, of calcium nitrate tetrahydrate $(Ca(NO_3)_24H_2O)$ are dissolved in 70 ml of distilled water. When needed, the admixtures are added at 1% vol of the starting solution. The flask is equipped with a dropping funnel, a pH meter, a conductimeter and the fourth neck is connected to an automatic titrator. Under magnetic stirring the aluminium sulphate solution (see above) is slowly added with the dropping funnel while the pH is kept constant to the desired value with a suspension of 40 g/l of calcium oxide (CaO) automatically dropped by the titrator. The addition of CaO ends when the final volume is reached.

Crystal morphology was observed, without any previous treatment, using an Environmental Scanning Electron Microscope equipped with a field emission gun (Philips XL30 ESEM-FEG) that allowed to obtain a much higher brilliance of the electronic source than the one of an ordinary SEM and to work in ESEM conditions (5 Torr, voltage: 10kV, T= 5°C).

In these working conditions free water is pumped away, while salt saturated water, the one in crystalline phases or in gel-like structures is preserved.

X-ray analyses were performed on powder obtained filtering the precipitate under vacuum, quenching it wit h methyl alcohol and then drying it. The mineral composition of each synthesis was determined by X-ray diffraction analysis. The XRPD data were collected at room temperature on a laboratory diffractometer (PANalytical X'pert PRO MPD equipped with an X'celerator detector), in continuous mode, with fixed slits and with CuKα radiation at 40 kV and 40 mA, calibrated against standard NAC. A 2θ step of 0.008° and a measuring time of 35 seconds per step were chosen to obtain a good signal/noise ratio. All the spectra were processed with the Maud software (Material Analysis Using Diffraction) [10] using the structural model proposed by Moore and Taylor [11] in order to refine lattice parameters.

2.2 Cementitious systems

Two binders were used to follow the hydration reactions.
The first one was prepared mixing a 90% of white Portland cement plus a 10% of aluminous cement (PTL). The pH starting value of PTL system was 12.5
The second one was prepared mixing a 90% of an aluminous cement plus a 10% of white Portland cement (TW). The pH starting value for this system was 10.
For the experiment we mixed an 80% of binder plus a 20% of β-hemihydrate hydrated with a w/p= 0,4. The amount of hemihydrate is intentionally high in order to increase the quantity of available sulphate in solution to maximize the production of ettringite during the very early stages of hydration.
We performed x-ray powder diffraction experiments at the European Synchrotron Radiation Facility (ESRF) beamline BM08 (GILDA). The instrumentation has been described elsewhere in detail [12].
The experiments were performed during a period of time of 12 hours taking samples from the same batches of cement, conserved in a sealed case, in order to follow the reaction without altering the behaviour of the cement blend in all measurements and avoiding to quench the sample. Up to now, actually, there is no reliable information available if and how the quenching procedures could modify the crystalline structures of the system involved.
The samples were prepared in a flat sample-holder and covered with a Kapton layer, to prevent the dehydration and carbonatation during the 10 minutes of data collection time.
X-ray diffraction patterns were accumulated on a flat image plate (IP) detector. The images collected on the IP were retrieved using the Fuji BAS2500 scanner, and the powder spectra were integrated and corrected using a specially developed software.
The experiments were performed at a relative humidity of 100% and at room temperature.
The wavelength used was 0.489197 Å calibrated against standard LaB_6. The angular range explored was 1-32° 2 theta corresponding to a d-spacing interval of 14 - 0,89 Å.
The collected spectra were elaborated with Rietveld method using the GSAS software [13] to obtain structural and quantitative information. The refinements were performed using structural models, for all the phases, taken from Inorganic Crystal Structure Database (ICSD). All the cementitious raw materials were commercially available products.

3. Results and discussion

3.1 Morphology of synthetic ettringites

Morphological information on synthetic ettringites was exclusively obtained from ESEM investigation. On these images we estimate the length/thickness ratio of the needles to try to correlate the chemical parameters of the synthesis, the broadening of the diffraction peaks and the lattice parameters.

3.1.1 pH influence

As described in the experimental section, we synthesized ettringite maintaining a constant pH value during the reaction. Three pH values, 10, 11, 12 have been chosen and three crystal morphologies could be observed (fig. 1).
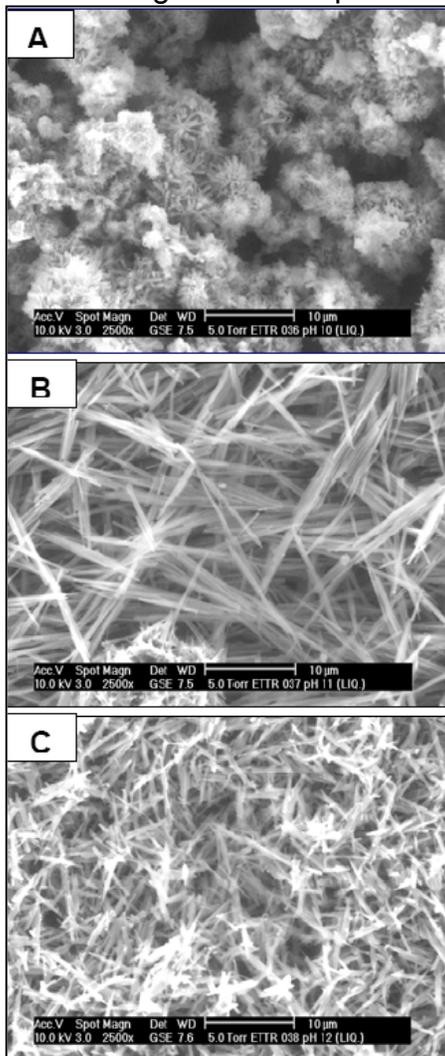
Length/thickness ratio of these ettringites has been measured treating the ESEM images with Image-Pro Plus 5.1 software and the results are reported in fig 2. A pH of 11 seems to promote the crystal growth and crystals exhibit a large length/thickness ratio. A change of pH to 10, led to smaller spherical aggregates of thin needles while a pH of 12 produces the formation of ettringite needles with intermediate sizes.

The increase of the pH value above 12 determines an increase of negative charges on surface of crystals. Coupled with a larger surface area this could lead to a colloidal ettringite with larger repulsion forces [14]. These characteristics cause the crystals to attract a large number of water molecules to the surface which in turn causes interparticle repulsion, possibly of double layer type [15].

Figure 1 Synthesis of ettringite at (A) pH 10 (B) pH11 (C) pH 12. Bar = 10 μm
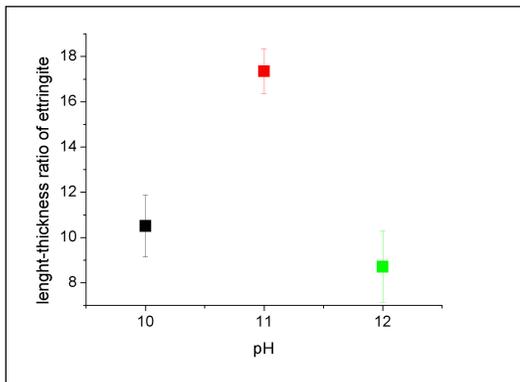
Figure 2. Length/thickness ratio of ettringite synthesized at different pH.

3.1.2 Salt concentration effect and presence of admixtures

Different concentration of calcium ions were examined because a variation of [Ca^{2+}] is expected during the hydration of a real cementitious system.
Furthermore, we tested the effect of three acrylic based superplasticizers (SP-A, SP-B, SP-C) usually added as high water reducers.
Notice that all the synthesis have been made at a constant pH of 11.
ESEM images of these synthesis are shown in fig 3 and 5.
A low or null salt concentration in excess into the starting solution (fig 3, A-B) give dense spheres with thin and short needles while a higher salt concentration gives long, fiberlike needles that become thicker and shorter as the [Ca^{2+}] ions increase into the starting solution. This is reported in fig. 4, where the length/thickness ratio is plotted against calcium concentration.
Notice the presence of an amorphous gel-like matrix between the crystals, that appear specially at high salt concentration (fig. 3, E).
Mehta [15] observed that ettringite that forms in the presence of lime is submicronic and has significantly higher surface area than the needle-shaped ettringite that forms when no lime is present.
The superplasticizers work on morphology affecting the nucleation process, giving numerous extremely thin and elongated crystals, pointing out the dispersing effect of these admixtures (fig. 5).
Information about length/thickess ratio of these synthesis are shown in fig. 6, in which SP-A seems to favourite larger crystals than SP-B, while SP-C has got an intermediate ratio.
It is believed that these differences in the morphological structures of the crystals could be the reason for the different behaviour in term of rate of hydration and mechanical strength development observed with the use of these polymers. Smaller ettringite crystals, formed when SP-B is used, could be more unstable and reactive in comparison with larger ones obtained with SP-A, allowing a faster development of mechanical strength [16].
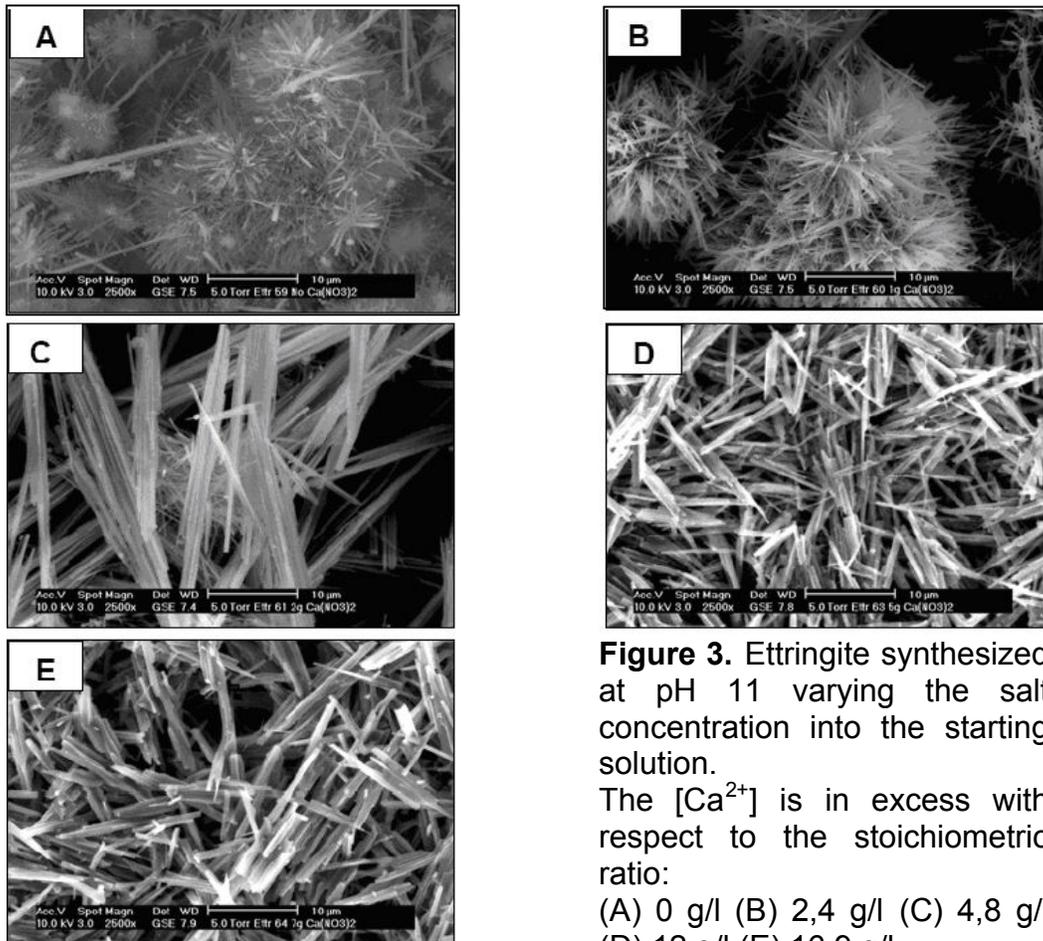
Figure 3. Ettringite synthesized at pH 11 varying the salt concentration into the starting solution.
The [Ca^{2+}] is in excess with respect to the stoichiometric ratio:
(A) 0 g/l (B) 2,4 g/l (C) 4,8 g/l (D) 12 g/l (E) 16,9 g/l.
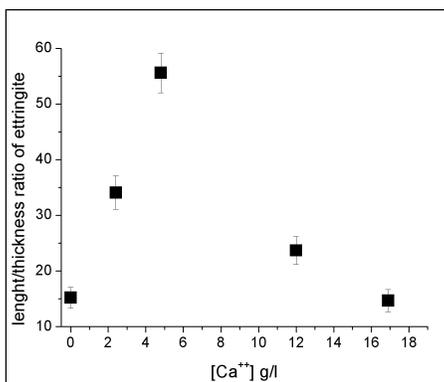
Figure 4. Length/thickness ratio of ettringite synthesized at pH11 with different [Ca^{2+}] in the starting solution
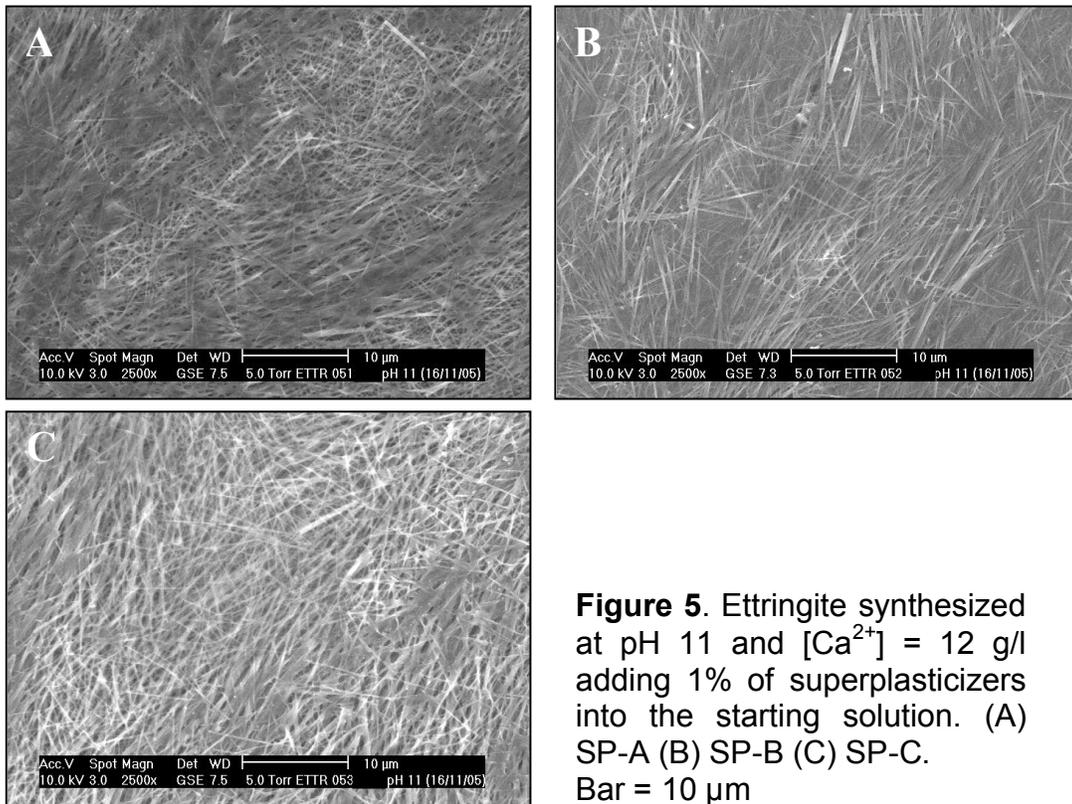
Figure 5. Ettringite synthesized at pH 11 and $[Ca^{2+}]$ = 12 g/l adding 1% of superplasticizers into the starting solution. (A) SP-A (B) SP-B (C) SP-C.
Bar = 10 µm
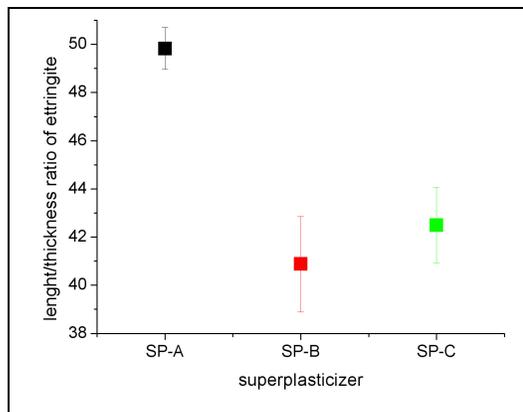
Figure 6. Length/thickness ratio of ettringite synthesized at pH 11 and $[Ca^{2+}]$ = 12 g/l adding a superplasticizer.

3.2 Refinement of lattice parameters of synthetic ettringites

Maud is a program for extraction of information on the microstructure of polycrystalline materials from X-ray diffraction data. Using this program all XRD patterns of synthetic ettringites were refined and mean values of a- and c- lattice parameters were determined.

Information about crystallite sizes of ettringite from different synthesis has also been collected.

Figure 7 is a plot of the c/a ratio and crystallite sizes of ettringite obtained in pH controlled conditions. Comparing this diagram with the one described in Figure 2, we can find a good agreement between morphology, lattice parameters and dimension of crystallites.
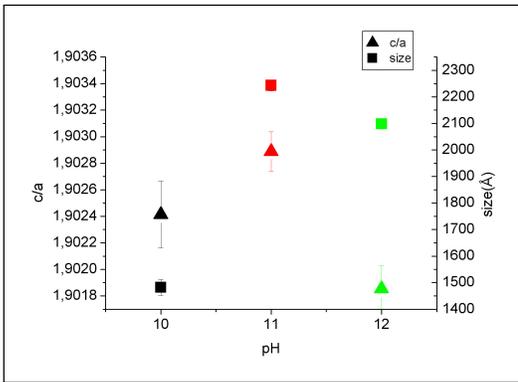
Figure 7. c/a ratio and crystallite size of ettringite synthesized with a constant pH value

These three parameters show a different relation when we synthesize ettringite varying the calcium concentration as reported in figures 4 and 8 (A and B).

About structural information, it can be noticed a decreasing of c/a ratio and a proportional growth of crystallites size as the amount of Ca^{2+} increases. In the same diagram has been also plotted the data obtained for additivated synthetic ettringites.

The effect given by the three superplasticizers on lattice parameters and crystallite dimensions are reversed if compared with the relation found studying the length/thickness ratio of the crystals (Fig. 6) as shown in fig. 8.

The reasons of the different influence of pH, salt concentration and admixtures on morphology and structure of the crystals are not yet fully understood.
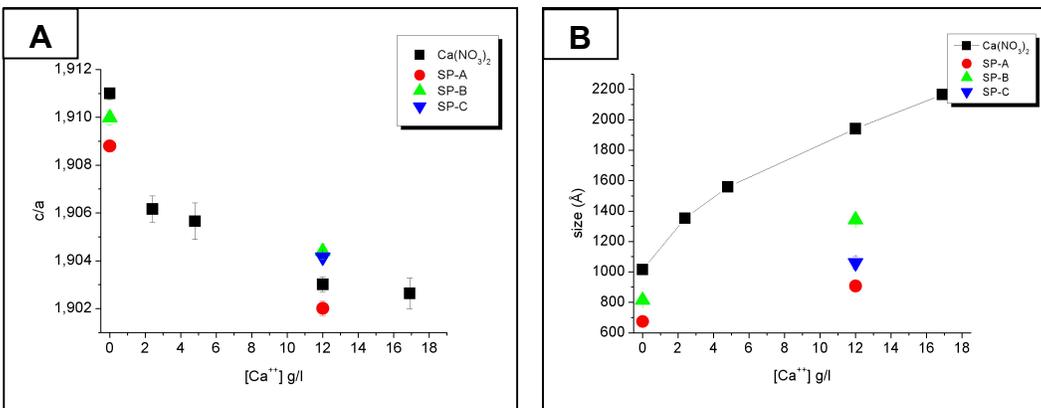
Figure 8. c/a ratio (A) and crystallite size (B) of ettringite synthesized varying the salt concentration in the starting solution with (coloured symbols. Red: SP-A, green: SP-B, blue: SP-C) and without (black squares) superplasticizers.

3.3 Ettringite in cementitious systems: synchrotron radiation x-ray diffraction

Synchrotron radiation x – ray diffraction was used to investigate the properties of ettringite developing in cements during the hydration process and in pH conditions comparable to those used during the synthesis reactions. Lattice parameters were obtained from Rietveld refinements.
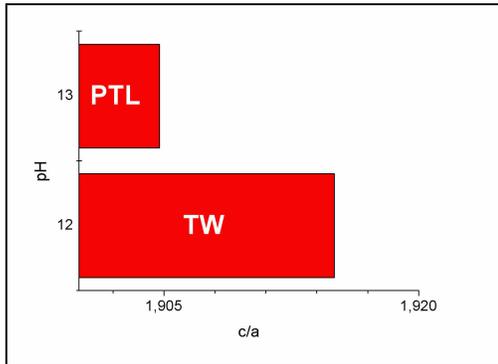
Figure 9. c/a ratio of ettringite vs pH measured after 120 minutes from the beginning of hydration of PTL and TW binders.

In Fig. 9 the bar graph shows the c/a ratio of ettringite, measured after 120 minutes from the beginning of hydration, of PTL and TW systems , where the pH value is about 13 and 12 respectively. The c/a values obtained can be evaluated comparing them with those calculated for ettringite synthesized in our laboratories in similar pH conditions.

These data are in very good agreement with the literature [8] and with the formation of sub-micron crystals at high pH.

Taking to account a- and c- parameters separately during the hydration time of PTL system, it can be noticed an increase of a and a decrease of c.

Barnes et al [17] explained the increasing of a- ascribing it to a variation of SO_3/OH (or H_2O) ratio into the structure considering that pure hydroxyl-ettringite has smaller molar volume. About the c- parameter, a possible explanation could be different $[Ca^{2+}]$ into to the column described before, or the presence of OH groups that can substitute oxygen into the coordination polyhedra.

In fig 10, is a plot of lattice parameters of ettringite in PTL system against time, together with the curve describing the crystallization of portlandite $(Ca(OH)_2)$ that starts to precipitate when the critical concentration of Ca^{2+} is reached.

If we compare this graph with the one in fig. 11, where the a- c- parameters of ettringite synthesized with an increasing amount of calcium are plotted, we can find a similitude especially as far as c- is concerned.

Actually, we can observe the same decreasing trend for this parameter in both synthetic and real ettringite while the Ca^{2+} concentration increases. As soon as portlandite forms, leading to a reduction of free calcium in solution, c-parameter of ettringite in the real system, seems to stabilize.

a- parameter, on the other hand, appears to be more influenced by some other factors a part from pH and [Ca^{2+}], such as the hydration of the other phases of cement and the action of soluble alkalis (Na, K) concentration.
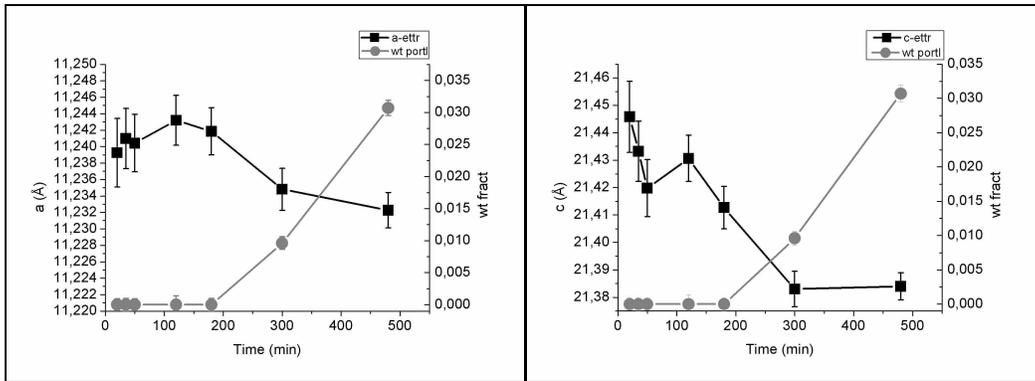
Figure 10. Variation of *a*- and *c*- parameters of ettringite in PTL system during the hydration process (black points). In grey, weight fraction of portlandite plotted against time.
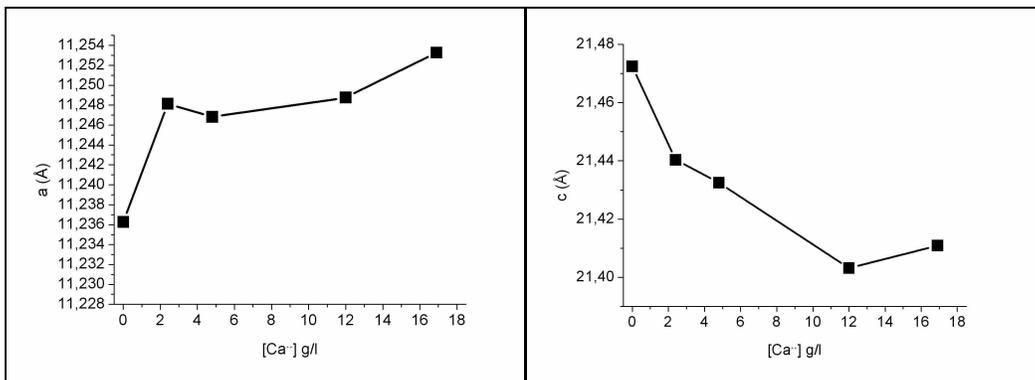
Figure 11. Variation of *a*- and *c*- parameters of synthetic ettringite plotted against [Ca^{2+}].

4. Conclusions

This work showed that morphology and microstructure of synthetic ettringite are influenced by pH, ionic strength and the presence of admixtures. Preliminary results on real cementitious systems showed a good agreement with the synthetic model.
Further study is needed to determine if these modifications can affect the setting behaviour and the mechanical strengths during early hydration stages.

References

[1] J. Stark, Delayed Ettringite Formation in Concrete. Proc. 17th Nordic Research Meeting. Ed.: Technical Committee. Reykjavik. Publ.: Betongforening. Oslo (1999) 4-28.

[2] F. W. Locher, W. Richartz, S. Sprung, W. Rechenberg: Erstarren von Zement. Teil IV: Einfluß der Lösungszusammensetzung. Zement-Kalk-Gips, 36 (1983) 4, 224- 231.

[3] P. K. Mehta, Mechanism of Sulphate Attack on Portland Cement Concrete - Another Look, Cem. and Concr. Res. 13 (1983), 401-406.

[4] W. Wieker, C. Hübert, H. Schubert, Untersuchungen zum Einfluß der Alkalien auf die Stabilität der Sulfoaluminathyrate in Zementstein und -mörteln bei Warmbehandlung. Schriftenreihe des Institutes für Massivbau und Baustofftechnologie, Uni Karlsruhe (1996), 175-186.

[5] A. Gabrisova, J. Havalica, S. Sahu, Stability of Calciumsulfoaluminate Hydrates in Water Solution with Various pH Values. CCR 21 (1991) 6, 1023-1027.

[6] I. Chartschenko, Theroretische Grundlagen zur Anwendung von Quellzementen in der Baupraxis. Habilitationsschrift, HAB Weimar (1995).

[7] M. Collepardi, Scienza e tecnologia del calcestruzzo, Hoepli, Milano (1991)

[8] L. J. Struble, P. W. Brown, An evaluation of ettringite and related compounds for use in solar energy storage: National Bureau of Standards, Progress Report, NBSIR 84-2942, (1984) 42 p.

[9] H. F. W. Taylor, Cement Chemistry, Academic Press, New York (1990)

[10] The Maud program, http://www.ing.unitn.it/~luttero/maud

[11] A. E. Moore and H.F.W. Taylor. Crystal Structure of Ettringite, Acta Crystallogr., B26, (1970), 386-393.

[12] C. Meneghini,G. Artioli, A. Balerna, A. F. Gualtieri, P. Norby, S. Mobilio, J. Synchrotron Rad. 8 (2001) 1162.

[13] A. C. Larson and R.B. Von Dreele, "General Structure Analysis System (GSAS)", Los Alamos National Laboratory Report LAUR 86-748 (2000).

[14] M. Constantinides, Preliminary Examination, http://www.ce.berkeley.edu/~margarit/PrelimReport.pdf

[15] PK Mehta, "Scanning Electron Microscopic Studies of Ettringite Formation." Cem. Concr. Res., 6 [2] (1976),169-82.

[16] T. Cerulli, P. Clemente, M. Decio, G. Ferrari, M. Gamba, D. Salvioni, F. Surico : A new Superplasticizer for Early High-Strength Development in Cold Climates, Proc. 7th CANMET/ACI International Conference on Superplasticizers and Other Admixtures in Concrete, Oct. 20-24, 2003, Berlin, Germany 113-124.

[17] P. Barnes, et al., The use of synchrotron sources in the study of cement materials, in: J. Bensted, P. Barnes (Eds.), Structure and Performance of Cements, Spon Press, London, (2002).